Talanta 101 (2012) 128–134

Contents lists available at SciVerse ScienceDirect

Talanta

journal homepage: www.elsevier.com/locate/talanta

A novel fluoride-selective electrode based on metalloporphyrin grafted-grapheneoxide

T. Poursaberi [a], M.R. Ganjali [b,*], M. Hassanisadi [a]

[a] Research Institute of Petroleum Industry, Tehran, Iran
[b] Center of Excellence in Electrochemistry, Faculty of Chemistry, University of Tehran, Enqelab Street, Tehran, Iran

ARTICLE INFO

Article history:
Received 25 June 2012
Received in revised form
26 August 2012
Accepted 27 August 2012
Available online 3 September 2012

Keywords:
Graphene oxide
Fluoride
Selective electrode
Metalloporphyrin
Potentiometry

ABSTRACT

In this work, the unique properties of graphene oxide were combined with the anion selectivity of metalloporphyrin to fabricate a novel fluoride-selective sensor. The electrode made of 27% PVC, 54% NPOE, 4% NaTPB and 15% NbTPP–GO was found to show the most favorable behavior. The sensor shows a Nernstian response (58.3 mV decade^{-1}) in the concentration window of 5.0×10^{-1}–5.0×10^{-7} mol L^{-1}with detection limit of 8.0×10^{-87} mol L^{-1}. The response of the sensor was found to be stable in the pH range of 3.0–7.0 and the metalloporphyrin grafted-GO based F^- sensors displayed very good selectivity with respect to a number of anions. The proposed sensor displays a long life time (more than 12 weeks) with a short response time of about 20 s.

1. Introduction

Since the start of the graphene revolution in 2004, it has captured increasing attention and has shown great promise in many applications [1–17], arising from its unique physicochemical properties such as high surface area, excellent thermal and electrical conductivity, electron mobility at room temperature, strong mechanical strength and flexibility [18–23]. The special properties of graphene may provide insight to fabricate novel potentiometric sensors for virtual applications. The excellent conductivity and small band gap are favorable for conducting electrons [23]. Graphene-based sensors can also have a much higher sensitivity because of the low electronic noise from thermal effect [24,25]. Furthermore, compared with CNTs, graphene can be obtained easily by chemical conversion of the inexpensive graphite [26]. Graphene oxide (GO) sheets are chemically exfoliated graphite oxide sheets with carboxylic groups at the edges and phenol, hydroxyl and epoxy groups on the basal planes [27]. Chemically functionalized graphene can be readily mixed with polymers in solution to form a stable dispersion and yield novel types of electrically conductive nanocomposites [28–30].

When incorporated into plasticized PVC membranes, metalloporphyrins become one of the most important classes of ionophores which induce unique anion selectivities [30–38]. Observed selectivity pattern for such membrane electrodes, e.g. chloride (In(III)-porphyrin [39]), thiocyanate (Mn(III)-porphyrin [40]), nitrite (Co(III)-porphyrin [41]), fluoride (Ga (III), Al(III) and Zr(IV)-porphyrins [42–50]), which often deviate significantly from the classical Hofmeister sequence, results from selective interaction of analyte anion with the metal center of the porphyrin structure. To the best of our knowledge, there is no report of the use of metalloporphyrin-grafted graphene for anion recognition in the literature, so fabrication of a new kind of sensor is possible through combination of the advantages of metalloporphyrins and graphene.

In this paper, the niobium (V)-metalloporphyrin grafted-graphene oxide was prepared and coated on platinum wire. An exciting advance was made in the field of ISEs by Freiser [51] when they developed coated wire electrodes (CWEs). Potentiometric sensors prepared by coating electroactive species on metallic or graphite conductors [52,53], with no internal electrolyte solution. They have been shown to be very effective for a wide variety of inorganic and organic anions and cations. These kinds of electrodes are very simple, durable, inexpensive and provide a reliable response over a wide concentration range [54]. The proposed electrode which is used for fluoride sensing, exhibited a great sensitivity as compared with the previously reported ones. Fluoride is one of the most hydrophilic anions ($\Delta G_{hyd}=-465$ kJ/mol [55]), therefore design of an ionophore which is selective towards fluoride ion is quite challenging. Compared to other anions selection of an ionophore for its

* Corresponding author. Tel.: +98 21 61112788; fax: +98 21 66495291.
E-mail address: ganjali@khayam.ut.ac.ir (M.R. Ganjali).

0039-9140/$ - see front matter © 2012 Elsevier B.V. All rights reserved.
http://dx.doi.org/10.1016/j.talanta.2012.08.039

successful detection is central, since it has to form a very strong complex with F^-. To obtain a non-Hofmeister selectivity pattern, this hydration energy should be overcome. In this way we open up a new avenue for fabricating excellent potentiometric sensors.

2. Experimental

2.1. Materials

Reagent grade o-nitrophenyl octyl ether (NPOE), dibutyl phthalate (DBP), diethyl sebacate (DES), sodium tetraphenylborate (NaTPB), hexadecyltrimethylammonium bromide (HTAB), tetrahydrofuran (THF), *N*,*N*-dimethylformamide (DMF), and high relative molecular weight PVC (all from fluka) were used as received. Nature flake graphite was purchased from Sigma-Aldrich. Nb (V)-5-4 (aminophenyl)-10, 15, 20-triphenyl porphyrin was synthesized and purified as described elsewhere [56–58]. H_2SO_4, $KMnO_4$, $NaNO_3$, NaF, H_2O_2, $SOCl_2$, triethylene amine and $CHCl_3$ were purchased from Sigma-Aldrich. Triply distilled deionized water was used throughout.

2.2. Equipments

XRD patterns of the solid products were obtained in the 2θ range of 5°–80° using a PW-1840 diffractometer from Philips Co. with Cu-Kα radiation ($\lambda = 1.54178$ Å). The thermograms of the samples were carried out between 25 and 700 °C at a heating rate of 10 °C/ min, using Mettler Toledo TGA/SDTA 851 instrument. FTIR spectra were obtained using a Vertex 70 FT-IR spectrophotometer from Bruker Co. to identify the functional groups and chemical bonding of the materials. UV–vis spectra were measured with a Carry 5030 spectrophotometer from Varian Co. A Corning ion analyzer 250 pH/mV meter was used for potential measurements at 25.0 ± 0.1 °C.

2.3. Ionophore preparation

Synthesis of Nb-TPP covalently bonded to graphene oxide molecules via an amide bond (NbTPP–GO, Fig. 1) was carried out in two stages:

2.3.1. Preparation of graphene oxide

GO was synthesized with the Hummers method [59]. Nature flake graphite was added to a flask with 50 mL of 98% H_2SO_4 in an ice bath, followed by slow addition of $KMnO_4$ and $NaNO_3$ under stirring. Then, deionized water was added and the temperature was raised to 98 °C. H_2O_2 was subsequently added into the flask. After cooling of the resultant mixture to room temperature, the mixture was filtrated and the filtered product was dried overnight at 60 °C. The product was suspended in water to yield a brown dispersion and subjected to dialysis to remove residual metal ions and acids. The purified dispersion was sonicated for 1.5 h at 300 W to exfoliate the GO, and unexfoliated GO was removed by centrifugation (4000 rpm, 5 min). At last, the GO sheets were obtained.

2.3.2. Synthesis of NbTPP–GO

According to the Xu et al. method [60] under argon atmosphere, graphene oxide was refluxed in $SOCl_2$ in the presence of DMF at 70 °C for 24 h. At the end of the reaction, excess $SOCl_2$ and solvent were removed by distillation. In the presence of triethylamine and under argon atmosphere, the above product was allowed to react with NbTPP in DMF at 130 °C for 72 h. To precipitate the product, the solution was cooled to room temperature and poured into ether. The product was isolated by filtration on a membrane (0.22 μm). The excess NbTPP and other impurities were removed through five washing cycles, which included sonication, filtration (discarding the filtrate), and re-suspension of the solid in THF. Then the precipitate was washed with $CHCl_3$. Afterwards the NbTPP–GO was washed with a small quantity of water to remove triethylamine, and finally dried under vacuum.

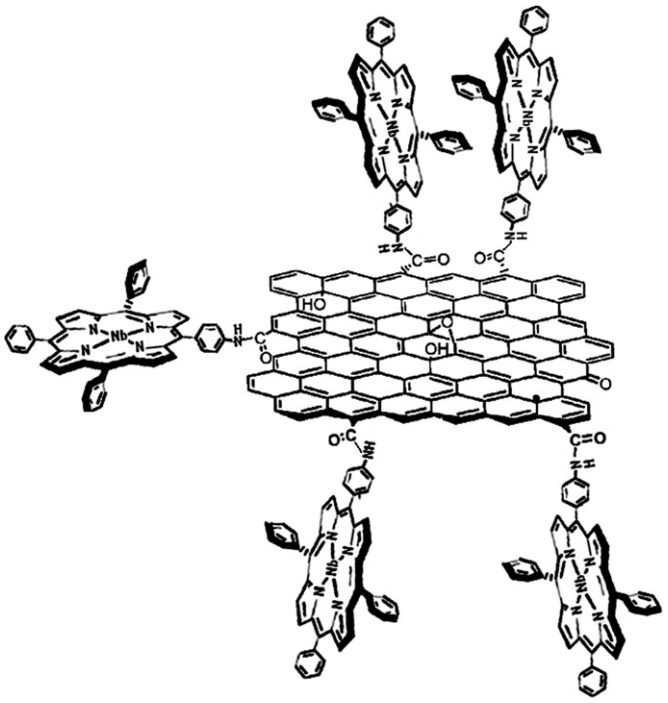

Fig. 1. Schematic representation of the NbTPP–GO.

2.4. Fabrication of the CWE

Membrane solution were prepared by thoroughly dissolving 27 mg powdered PVC, 15 mg ionophore NbTPP–GO, 4 mg NaTPB and 54 mg plasticizer NPOE in 5 mL of THF. The resulting mixture was transferred into a glass dish of 2 cm diameter. Coating process of CWEs was performed by dipping each platinum wire five times into this mixture. After each coating the membrane was air-dried for 12 h until a thin film was formed. The electrode was finally conditioned for 1 h in a 10^{-2} M of NaF solution.

2.5. Emf measurement

All measurements of emf were made at 25 ± 0.1 °C by use of the following assembly:

Pt wire/membrane/sample solution/Hg–Hg_2Cl_2, KCl (satd.)

A Corning ion analyzer 250 pH/mV meter was used for potential measurements. The emf observations were made relative to a double-junction saturated calomel electrode (SCE, Philips) with the chamber filled with an ammonium nitrate solution. The performance of the electrodes was investigated by measuring the emfs of sodium fluoride solutions prepared with concentration range 10^{-1}–10^{-8} mol L^{-1} serial dilution. Each solution was stirred and the potential reading was recorded when it became stable (change within 1–2 mV), and then plotted as logarithmic function of F^- activity. Activities were calculated according to the Debye–Huckel procedure [61].

3. Results and discussion

3.1. Structural characterization

The X-ray diffraction (XRD) patterns of graphite and GO are shown in Fig. 2. The pattern of pure graphite shows a peak at 26.6° corresponding to a basal spacing d_{002}=3.34 Å. In comparison to the natural graphite, a wide peak is observed for GO at 12.0° corresponding to a basal spacing of d_{001}=7.33 Å. [62,63] because of the presence of intercalated H_2O molecules and various oxide groups (Fig. 2) [64] which clearly indicates the damage of the regular crystalline pattern of graphite during the oxidation [65].

In order to understand the interaction between NbTPP and GO, FTIR spectrum was recorded (Fig. 3). It is seen that the GO sheets carried adsorbed water molecules and structural OH groups (a strong absorption band at 3410 cm^{-1} due to O–H stretching vibrations), C=O (the C=O stretching vibrations from carbonyl and carboxylic groups at 1734 cm^{-1}), and C–O (C–OH stretching vibrations at 1200 cm^{-1} or O–C–O stretching vibrations at 1050 cm^{-1}) groups, indicated the attachment of oxo-groups on GO sheets after the chemical oxidation of the flake graphite. The spectrum also showed a band around 1520 cm^{-1} corresponding to the C=C stretching vibrations of carbon–carbon bonds in the aromatic ring. In the spectrum of NbTPP–GO, the peak at 1734 cm^{-1} almost disappeared, and a new band emerged at 1640 cm^{-1}, which corresponds to the C=O characteristic stretching band of the amide group. The stretching band of the amide C–N peak also appeared at 1260 cm^{-1}. These results clearly proves that the Nb (V)-porphyrin complex has covalently attached to the carboxylic groups of GO through the formation of a stable amide bond.

The thermal property and the composition of the GO and NbTPP–GO were characterized by TG analysis (Fig. 4). As shown in Fig. 4.a, there are three steps for mass losing upon temperature increments. The mass loss at around 100 °C could be ascribed to the removal of adsorbed water. The mass loss at around 200 °C was attributed to the decomposition of labile oxygen functional groups [66]. The mass loss at around 500 °C was ascribed to the carbon combustion [63]. The weight-loss stage in the region of 330–380 °C of NbTPP–GO TGA curve may result from the decomposition of metalloporphyrins [67–69]. These data showed that modification of GO nanoparticles with metalloporphyrin has been performed and they have been bonded to each other chemically.

3.2. Stability constants of different anion-NbTPP complexes

Previous studies showed that the metalloporphyrin complexes containing different central metal exhibit different anion selectivity [30–38]. Thus, at first we carried out some spectrometric measurements in acetonitrile–water (1:1, v/v) solution in order to obtain quantitative information about the anion–NbTPP interactions. The NbTPP spectrum (Fig. 5) exhibited a strong Soret absorption at 420 nm, and weak Q-bands between 500 and

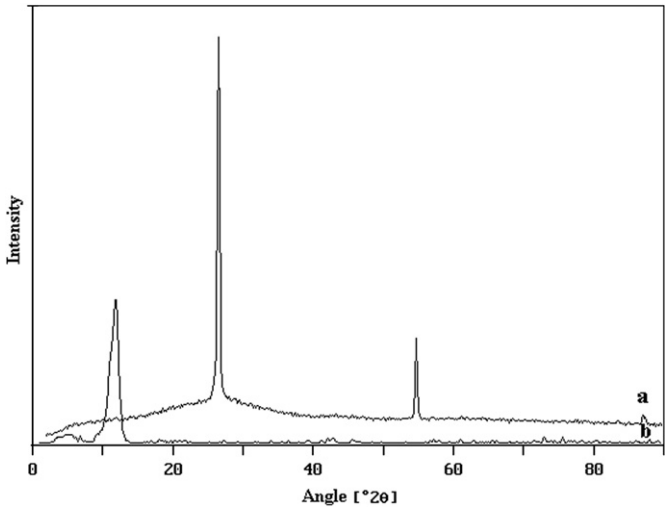

Fig. 2. XRD patterns of graphite (a) and GO (b).

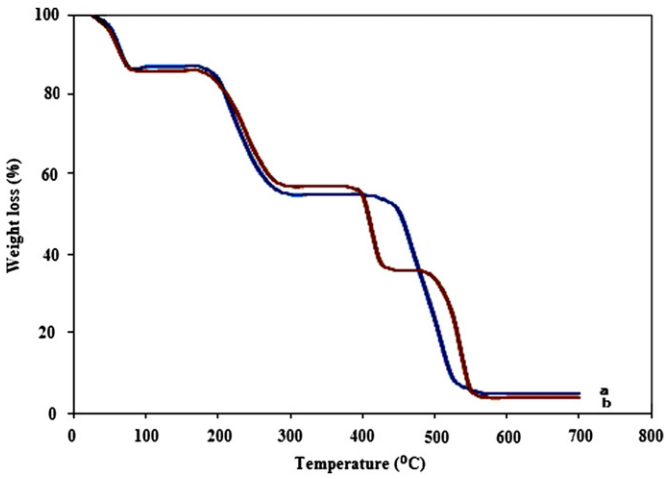

Fig. 4. TGA curves of GO (a) and NbTPP–GO (b).

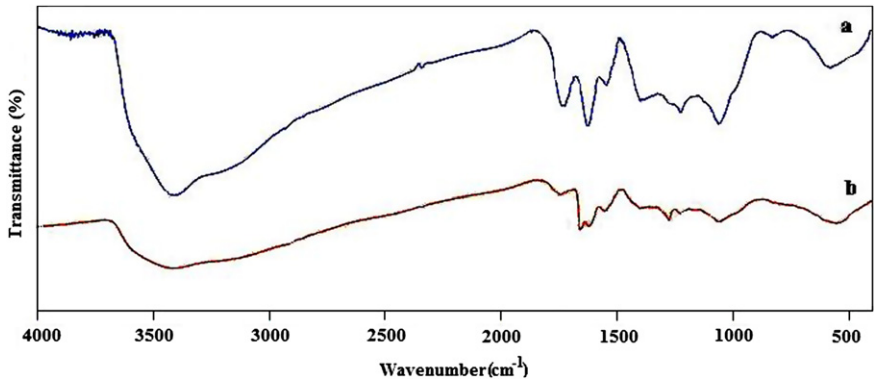

Fig. 3. FT-IR spectra of GO (a) and NbTPP–GO (b).

700 nm, which were consistent with that of TPP-NH2 analogues [70]. The addition of fluoride ion to a NbTPP solution resulted in a increase in Soret absorption and the formation of a stable 1:1 fluoride-NbTPP complex in solution. The formation constants ($\log K_f$) of the NbTPP and some anions are summarized in Table 1. As it is seen; there was a strong interaction between fluoride and NbTPP. This could be mainly due to the selective bonding of fluoride to the metal center which is thought to be the origin of the selectivity of NbTPP-based electrode for fluoride over other anions.

3.3. Effect of membrane composition

Different aspects of membrane preparation based on the NbTPP–GO for F^- ion were optimized and the results are summarized in Table 2. As seen with increasing NbTPP–GO content until a value of 15% (M_1–M_3) the sensitivity of electrode response has increased. However, further addition of ionophore, resulted in the diminished response of the electrode (M_4), most probably due to some inhomogeneities and possible saturation of the membrane. The potentiometric response of the membrane ion-selective electrodes was greatly influenced by the polarity of the membrane medium, which is defined by the dielectric constants of the major membrane components [71–73]. The influence of the nature of plasticizer on the F^- response was studied on electrodes. Three types of plasticizers having different dielectric constants, namely, DES, DBP, and NPOE were studied. As shown in Table 2 (M_3, M_5, M_6), NPOE with the highest dielectric constant in the series resulted in the best sensitivity of the potential responses. The response properties of anion-selective electrodes based on ion carriers were strongly influenced by the lipophilic ionic sites [74]. The response of ISE membrane in the presence of various ionic sites was used to determine whether the carrier has acted as electrically charged or uncharged. In cases in which a charged carrier mechanism (the ionophore is initially positively charged and becomes neutral upon subsequent ligation of an anion) was prevalent, anionic (typically tetraphenylborate derivates) sites were added to the polymer membrane. In this way a Nernstian response, diminution of the membrane resistance, lessening of the co-anion interferences, improvement of the detection limit and optimization of the selectivity could be obtained. However, when a neutral carrier mechanism (when the ionophore is initially neutral and becomes negatively charged when bound to a sample ion) was dominant, cationic (typically quaternary ammonium salts) sites were introduced. So, the possible response mechanism and the effect of additives on the potentiometric response of NbTPP-based ISE, was investigated by varying the nature and amount of ionic additives (M_3, M_7, M_8). Results in Table 2 showed that the addition of HTAB as a cationic additive had no significant effect on the slope and dynamic range of the calibration graph (compare M_3 and M_8). On the other hand, addition of NaTPB to the membrane (M_7) caused an increase in the slope of the calibration graph, which approached the Nernstian behavior (58.3 mv/decade). These results revealed that NbTPP in the membrane has acted as a positively charged carrier. In anion-selective electrodes based on positively charged carriers, ionic sites with the same charge sign as the primary ion was required to optimize selectivity. As is shown in selectivity studies, the selectivity of the membrane has improved upon addition of NaTPB and worsened in the presence of HTAB which was another evidence for the electrode functioning based on charged carrier mechanism. It should be also noted that when the plasticizer/PVC ratio was twice the best slope and linear dynamic range was obtained. Thus, the membrane M_7 with the optimized composition of NPOE:PVC:NbTPP–GO:NaTPB ratio of 54:27:15:4 was selected for the preparation of CWE for fluoride ion.

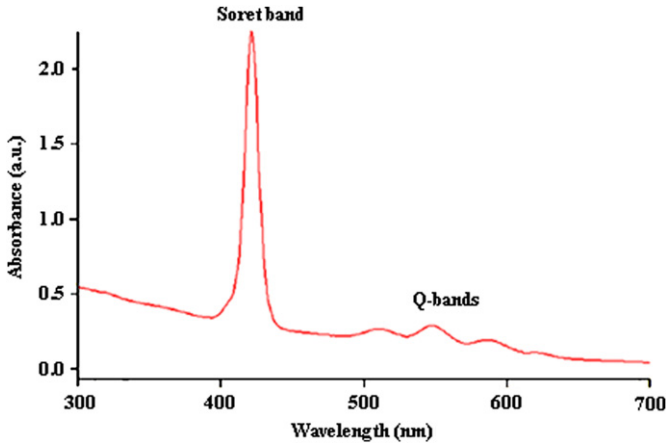

Fig. 5. Absorbance spectrum of NbTPP.

Table 1
Stability constants of anion-NbTPP complexes.

Aniona	$\log K_f$
F^-	5.40 ± 0.03
SCN^-	4.85 ± 0.03
ClO_4^-	4.72 ± 0.04
Cl^-	4.42 ± 0.02
Br^-	4.19 ± 0.05
NO_3^-	3.93 ± 0.04
I^-	3.58 ± 0.02
SO_4^{2-}	3.25 ± 0.03

Table 2
Effect of different membrane composition on fluoride selective electrode response, the membrane code M7 that indicated with box is the optimum membrane composition.

Membrane code	Composition (%)				Working range (M)	Slope (mVdecade^{-1})
	PVC	Plasticizer	Ionic site	Nb–TPP–GO		
M_1	30	65,NPOE	–	5	1.0×10^{-3}–5.0×10^{-5}	−35.2
M_2	30	60,NPOE	–	10	5.0×10^{-2}–1.0×10^{-5}	−45.3
M_3	30	55,NPOE	–	15	5.0×10^{-1}–1.0×10^{-5}	−53.5
M_4	30	50,NPOE	–	20	1.0×10^{-2}–1.0×10^{-6}	−46.5
M_5	30	55,DES	–	15	5.0×10^{-1}–5.0×10^{-6}	−45.4
M_6	30	55,DBP	–	15	1.0×10^{-2}–1.0×10^{-5}	−42.2
M_7	27	54,NPOE	4 NaTPB	15	5.0×10^{-1}–5.0×10^{-7}	−58.3
M_8	27	54,NPOE	4 HTAB	15	1.0×10^{-2}–5.0×10^{-5}	−45.7

3.4. Calibration curve

The EMF response of the proposed F^- sensor based on NbTPP–GO, prepared under optimal membrane ingredients, indicated a linear range from 5.0×10^{-1}–5.0×10^{-7} mol L^{-1} (Fig. 6). The slope of calibration curve was -58.3 ± 0.5 mV per decade. The limit of detection, as determined from the intersection of the two extrapolated segments of the calibration graph, was 8.0×10^{-8} M.

3.5. Effect of pH

The influence of pH of the test solution (1.0×10^{-3} mol L^{-1} fluoride) on the potential response of the membrane sensor was tested in the pH range of 2.0 to12.0 adjusted with either H_2SO_4 or KOH. The results, shown in Fig. 7, implied that the metal center of the complex was mainly responsible for the pH response of the membrane. In fact, OH^- and F^- ions coordinated competitively with the metal center of the ionophore. However the response of the electrode was hardly affected by pH changes in the range of 3.0–7.0. As the pH of solution increased, OH^- became the primary ion and consequently, the potentiometric response of the electrode for F^- ion deviated from linearity. Therefore, at low F^- concentrations, it was necessary to work at the more acidic region of the pH-potential response curve. To avoid the nearly complete protonation of F^- in sample solutions with lower pH (The pK_a of Hf acid is 3.15 so the concentration ratio of F^-/HF at pH 3.5 is 2.0) [75] and the interference of OH^- at higher pHs, pH 3.5 (Gly/HCl buffer) was chosen for further experiments. It should be noted that, since in this pH half of the fluoride anions were in protonated form, therefore the concentration used to plot calibration curve represent the free fluoride anion concentration, not the total fluoride added to the sample solution.

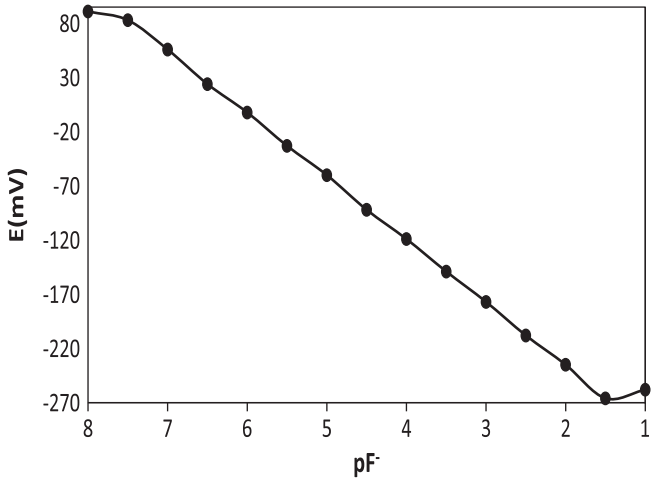

Fig. 6. Potential responses of F^--selective electrode based on NbTPP–GO.

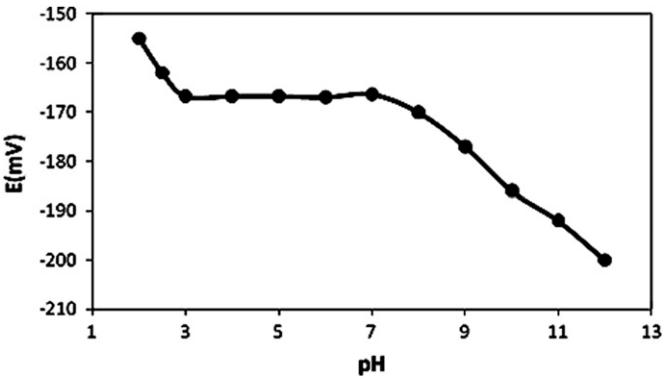

Fig. 7. Effect of pH of the test solution (1.0×10^{-3} mol $L^{-1}$of F^-) on the potential response of the F^-selective electrode.

3.6. Response time

Dynamic response time is an important factor for any ion-selective electrode. In this study, the practical response time of the F^--selective electrode was recorded by using solutions with different F^- concentrations. The measurements sequence was from the lower (1.0×10^{-7} M) to the higher (1.0×10^{-2} M) concentrations. The actual potential versus time traces is shown in Fig. 8. As it is seen, the response time for the electrode was about 20 s for dilute fluoride solutions ($<10^{-3}$ M) and at higher concentrations ($>10^{-3}$ M), response time was shorter ($\sim$10 s).

3.7. Life time

Lifetime study is based on monitoring the change in electrode slope and linear dynamic range with time. After 12 weeks a very slight gradual decrease in slope was observed (i.e., -57.9 mV per decade). The reproducibility of the sensor was tested. The standard deviation of potential measurements for 10 different solutions at 1.0×10^{-4} mol L^{-1} fluoride was ±1.4 mV.

3.8. Selectivity

The influence of interfering ion on the response behavior of ion-selective membrane electrode is usually described in terms of selectivity coefficients. Potentiometric selectivity coefficient values for the present sensor were determined by the match potential method (MPM) which is recommended by IUPAC [76,77]. According to this method, the specified activity (concentration) of the primary ion (A) is added to a reference solution, and the potential is measured. In a separate experiment, the interfering ion (B) is successively added to an identical reference solution until the measured potential matched that obtained before by adding the primary ions. The matched potential selectivity coefficients, is then given by the resulting primary ion to interfering ion activity (concentration) ratio. The experimental conditions employed and the resulting values are given in Fig. 9.

As it can be seen from Fig. 9, the electrode is very selective to fluoride ion and the observed selectivity pattern significantly differs from the so-called Hofmeister selectivity sequence. The order of anion selectivity of the electrode shown in Fig. 9

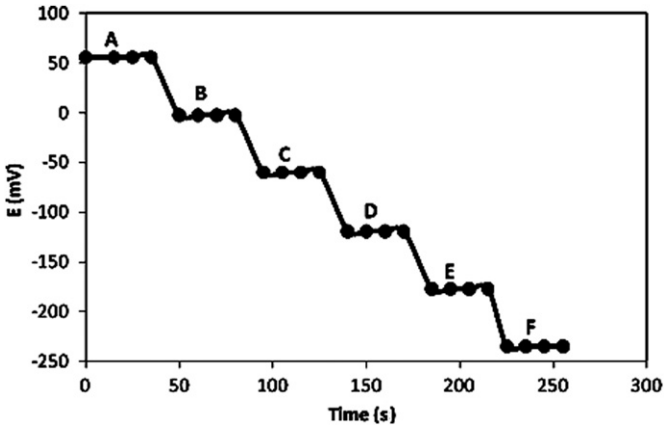

Fig. 8. Dynamic response of fluoride membrane electrode for step changes in concentration of F^- (A) 1.0×10^{-7}, (B) 1.0×10^{-6}, (C) 1.0×10^{-5}, (D) 1.0×10^{-4}, (E) 1.0×10^{-3} and (F) 1.0×10^{-2} M.

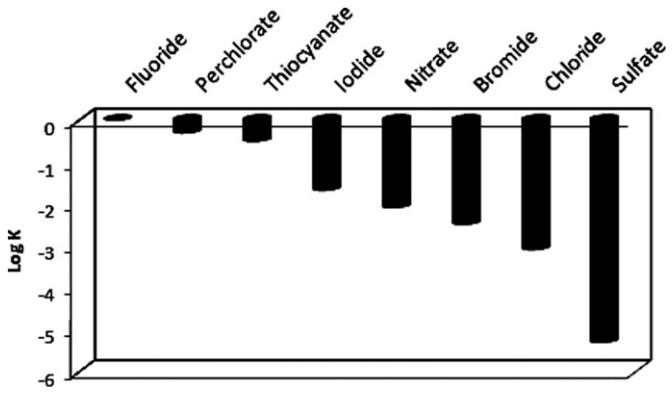

Fig. 9. Logarithm of selectivity coefficients for the F^--ion selective electrode. Experimental conditions: Reference solution (5.0×10^{-7} M of F^-), primary ion (1.0×10^{-6}–1.0×10^{-2} M of F^-), interfering ion (1.0×10^{-5}–1.0×10^{-1} M).

suggested that NbTPP–GO was not behaving as a classical dissociation ion-exchange molecule in the membrane. That is, there must be some association of the anion with the metal center in the complex, and the selective bonding of fluoride to this metal center is thought to be the origin of the selectivity of NbTPP–GO-based electrode for fluoride over other anions.

3.9. Analytical applications

To assess the precision and trueness of the measurements obtained with the proposed electrode; it was applied to determine F^- in BAM certified fluoride standard solution (Sigma-Aldrich). The result (1002 ± 14 mg/kg), derived from five replicate measurements, was found to be in satisfactory agreement with the stated fluoride content (1000 mg/kg).

Considering the practical applicability of proposed electrode for determination of F^- in real samples, it was also used in the determination of fluoride ions in mouth wash solution (Kimia Daru Co., Tehran, Iran). 1.0 g of sample was taken and diluted with distilled water in a 100 mL flask and the fluoride content of resulting solution was then determined by the proposed sensor using the calibration curve. The result of triplicate measurements was (2.02 ± 0.03)% which was in agreement with declared fluoride content (2.0%).

4. Conclusion

In this work, GO sheets were functionalized by Nb (V)-porphyrin and used as selective sensing element in construction of a coated wire electrode for the measurement of fluoride ions. The electrode based on GO and NbTPP showed superior performance over previous electrodes. The introduction of GO improved the dynamic working range, detection limit, response time, lifetime, and stability of the sensor. The electrode exhibited linear response over a wide concentration range of 5.0×10^{-7}–5.0×10^{-1} mol L^{-1} with a Nernstian slope of -58.3 mV decade^{-1}, and a short response time of 20 s.

References

[1] J. Hass, W.A. de Heer, E.H. Conrad, J. Phys. Condens. Matter. 20 (2008) 323202–323229.
[2] M.D. Stoller, S.J. Park, YW. Zhu, J.H. An, R.S. Ruoff, Nano Lett. 8 (2008) 3498–3502.
[3] E. Yoo, J. Kim, E. Hosono, H. Zhou, T. Kudo, I. Honma, Nano Lett. 8 (2008) 2277–2282.
[4] D.H. Wang, D.W. Choi, J. Li, Z.G. Yang, Z.M. Nie, R. Kou, D.H. Hu, C.M. Wang, L.V. Saraf, J.G. Zhang, I.A. Aksay, J. Liu, ACS Nano. 3 (2009) 907–914.
[5] B. Seger, P.V. Kamat, J. Phys. Chem. C 113 (2009) 7990–7995.
[6] R. Kou, Y.Y. Shao, D.H. Wang, M.H. Engelhard, J.H. Kwak, J. Wang, V.V. Viswanathan, C.M. Wang, Y.H. Lin, Y. Wang, I.A. Aksay, J. Liu, Electrochem. Commun. 11 (2009) 954–957.
[7] E. Yoo, T. Okata, T. Akita, M. Kohyama, J. Nakamura, I. Honma, Nano Lett. 9 (2009) 2255–2259.
[8] Y.C. Si, E.T. Samulski, Chem. Mater. 20 (2008) 6792–6797.
[9] Y.M. Li, L.H. Tang, J.H. Li, Electrochem. Commun. 11 (2009) 846–849.
[10] X. Wang, L.J. Zhi, N. Tsao, Z. Tomovic, J.L. Li, K. Mullen, Angew. Chem. Int. Ed. 47 (2008) 2990–2992.
[11] J.B. Wu, H.A. Becerril, Z.N. Bao, Z.F. Liu, Y.S. Chen, P. Peumans, Appl. Phys. Lett. 92 (2008) 263302/1-3.
[12] Z. Liu, J.T. Robinson, X.M. Sun, H.J. Dai, J. Am. Chem. Soc. 130 (2008) 10876–10877.
[13] H. Chen, M.B. Muller, K.J. Gilmore, G.G. Wallace, D. Li, Adv. Mater. 20 (2008) 3557–3561.
[14] C.S. Shan, H.F. Yang, J.F. Song, D.X. Han, A. Ivaska, L. Niu, Anal. Chem. 81 (2009) 2378–2382.
[15] Z.J. Wang, X.Z. Zhou, J. Zhang, F. Boey, H. Zhang, J. Phys. Chem. C 113 (2009) 14071–14075.
[16] C.H. Lu, H.H. Yang, C.L. Zhu, X. Chen, G.N. Chen, Angew. Chem. Int. Ed. 48 (2009) 4785–4787.
[17] Y. Wang, J. Lu, L.H. Tang, H.X. Chang, J.H. Li, Anal. Chem. 81 (2009) 9710–9715.
[18] A.K. Geim, K.S. Novoselov, Nat. Mater. 6 (2007) 183–191.
[19] S. Park, R.S. Ruoff, Nat. Nanotechnol. 4 (2009) 217–224.
[20] A.A. Balandin, S. Ghosh, W.Z. Bao, I. Calizo, D. Teweldebrhan, F. Miao, C.N. Lau, Nano Lett. 8 (2008) 902–907.
[21] R.F. Service, Science 324 (2009) 875–877.
[22] C. Lee, X.D. Wei, J.W. Kysar, J. Hone, Science 321 (2008) 385–388.
[23] S. Stankovich, D.A. Dikin, G.H.B. Dommett, K.M. Kohlhaas, E.J. Zimney, E.A. Stach, R.D. Piner, S.T. Nguyen, R.S. Ruoff, Nature 442 (2006) 282–286.
[24] Z.M. Ao, J. Yang, S. Li, Q. Jiang, Chem. Phys. Lett. 461 (2008) 276–279.
[25] N.M.R. Peres, F. Guinea, A.H.Castro Neto, Phys. Rev. B 73 (2006) 125411–125423.
[26] C. Xu, X. Wang, J.W. Zhu, J. Phys. Chem. C 112 (2008) 19841–19845.
[27] A. Lerf, H.Y. He, M. Forster, J. Klinowsk, J. Phys. Chem. B 102 (1998) 4477–4482.
[28] D. Li, R.B. Kaner, Science 320 (2008) 1170–1171.
[29] S. Niyogi, E. Bekyarova, M.E. Itkis, J.L. Mcwilliams, M.A. Hamon, R.C. Haddon, J. Am. Chem. Soc. 128 (2006) 7720–7721.
[30] H.C. Schniepp, J.L. Li, M.J. Mcallister, H. Sai, M. Herrera-Alonso, D.H. Adamson, R.K. Prud'homme, R. Car, D.A. Saville, I.A. Aksay, J. Phys. Chem. B 110 (2006) 8535–8539.
[31] V.K. Gupta, A.K. Jain, L.P. Singh, U. Khurana, Anal. Chim. Acta 355 (1997) 33–41.
[32] Y.U. Vlasov, A. Legin, A. Rudnitskaya, Sens. Actuat. B 44 (1997) 532–537.
[33] (a) M. Biesaga, K. Pyrzynska, M. Trojanowicz, Talanta 50 (2000) 209–224; (b) V.K. Gupta, A.K. Jain, R. Mangla, Sens. Actuat. B 76 (2000) 617–623.
[34] S. Sadeghi, M. Shamsipur, Anal. Lett. 33 (2000) 17–28.
[35] K. Seiler, W. Simon, Anal. Chim. Acta 266 (1992) 73–87.
[36] E.D. Steinle, U. Schaller, M.E. Meyerhoff, Anal. Sci. 14 (1998) 79–84.
[37] E.D. Steinle, S. Amemiya, P. Bühlmann, M.E. Meyerhoff, Anal. Chem. 72 (2000) 5766–5773.
[38] E. Malinowska, J. Niedziolka, M.E. Meyerhoff, Anal. Chim. Acta 432 (2001) 67–78.
[39] A.M. Pimenta, A.N. Araújo, M. Conceição, B.S.M. Montenegro, C Pasquini, J.R. Rohwedder, I.M. Raimundo, J. Pharm. Biomed. Anal. 36 (2004) 49–55.
[40] H. Ran Seo, H. Kyoung Lee, S. Jeon, Bull. Korean Chem. Soc. 25 (2004) 1484–1488.
[41] E. Fagadar-Cosma, D. Vlascici, G. Fagadar-Cosma, O. Bizerea, A. Chiriac, Rev. Chim. 55 (2004) 882–885.
[42] J.T. Mitchell-Koch, M. Pietrzak, E. Malinowska, M.E. Meyerhoff, Electroanalysis 18 (2006) 551–557.
[43] L. Gorski, M.E. Meyerhoff, E. Malinowska, Talanta 63 (2004) 101–107.
[44] E. Malinowska, L. Górski, M.E. Meyerhoff, Anal. Chim. Acta 468 (2002) 133–142.
[45] E. Steinle, U. Schaller, M.E. Meyerhoff, Anal. Sci. 14 (1998) 79–84.
[46] E. Malinowska, Ł. Gorski, M.E. Meyerhoff, Anal. Chim. Acta 468 (2002) 133–141.
[47] Ł. Gorski, M.E. Meyerhoff, E. Malinowska, Talanta 63 (2004) 101–107.
[48] M. Pietrzak, M.E. Meyerhoff, E. Malinowska, Anal. Chim. Acta 596 (2007) 201–209.
[49] D. Vlascici, O. Bizerea-Spiridon, E. Făgădar-Cosma, in: Proceedigns of the 13th Symposium on Analytical and Environmental Problems, Szeged, 25 September, 2006.
[50] Ł Gorski, E. Malinowska, Anal. Chim. Acta 540 (2005) 159–165.
[51] H. Freiser, J. Chem. Soc. Faraday Trans. 182 (1986) 1217–1221.
[52] Y.K. Lee, J.T. Park, C.K. Kim, K.Y. Whang, Anal. Chem. 58 (1986) 2101–2103.
[53] Y. Yang, Y. Bi, M. Liu, J. Fu, Z. Xi, Microchem. J. 55 (1997) 348–350.
[54] S. Kamata, A. Bhale, Y. Fukunaga, A. Murata, Anal. Chem. 60 (1998) 2464–2467.
[55] Y. Marcus, J. Chem. Soc. Faraday Trans. 87 (1991) 2995–2999.

[56] C. Sairam Sundaram, N. Viswanathan, S. Meenakshi, J. Hazard. Mater. 155 (2008) 206–215.
[57] S.A. Wasay, M.J. Haron, S. Tokunaga, Water Environ. Res. 68 (1996) 295–300.
[58] S. Meenakshi, C. Sairam Sundaram, Rugmini Sukumar, J. Hazard. Mater. 153 (2008) 164–172.
[59] W.S. Hummers, R.E. Offeman, J. Am. Chem. Soc. 80 (1958) 1339–1339.
[60] Y. Xu, Z. Liu, X. Zhang, Y. Wang, J. Tian, Y. Huang, Y. Ma, X. Zhang, Y. Chen, Adv. Mater. 21 (2009) 1275–1279.
[61] E. Bakker, Electroanalysis 9 (1997) 7–12.
[62] C. Nethravathi, B. Viswanath, C. Shivakumara, N. Mahadevaiah, M. Rajamathi, Carbon 46 (2008) 1773–1781.
[63] A.B. Bourlinos, D. Gournis, D. Petridis, T. Szabo, A. Szeri, I. Dekany, Langmuir 19 (2003) 6050–6055.
[64] H.K. Jeong, Y.P. Lee, M.H. Jin, E.S. Kim, J.J. Bae, Y.H. Lee., Chem. Phys. Lett. 470 (2009) 255–258.
[65] J. Zheng, X. Ma, X. He, M. Gao, G. Li, Proc. Eng. 27 (2012) 1478–1487.
[66] K. Kim, I. Kim, S. Park, Synthet. Metal. 160 (2010) 2355–2360.
[67] M.E. Kosal, K.S. Suslick, J. Solid. State Chem. 152 (2000) 87–98.
[68] J.H. Cai, J.W. Huang, P Zhao, Y.J. Ye, H.C. Yu, L.N. Ji, J. Sol–Gel Sci. Technol. 50 (2009) 430–436.
[69] M. Espinosa, E. Terres, S. Pacheco, R. Mejia, R. Rodriguez, J. Sol–Gel Sci. Technol. 53 (2010) 239–245.
[70] T. Umeyama, M. Fujita, N. Tezuka, N. Kadota, Y. Matano, K. Yoshida, S. Isoda, H. Imahori, J. Phys. Chem. C 111 (2007) 11484–11493.
[71] W.E Morf, The Principle of Ion-Selective Electrodes and Membrane Transport, Elsevier, New York, 1981.
[72] Y. Masoda, Y. Zhang, C. Yan, B. Li, Talanta 46 (1998) 203–213.
[73] M. Shamsipur, M. Yousefi, M.R. Ganjali, Anal. Chem. 72 (2000) 2391–2394.
[74] M. Lerchi, F. Orsini, Z. Cimerman, E. Pretsch, D.A. Chowdhury, S. Kamata, Anal. Chem. 68 (1996) 3210–3214.
[75] J.A. Dean (Ed.), Lange's Handbook of Chemistry, McGraw-Hill, New York, 1992.
[76] Y. Yang, Y. Bi, M. Liu, J. Fu, Z. Xi, Microchem.J. 55 (1997) 348–350.
[77] Y. Umezawa, K. Umezawa, H. Sato, Pure Appl. Chem. 67 (1995) 507–518.